Anomalous Thermoelectric Effects of $ZrTe_5$ in and beyond the Quantum Limit

J. L. Zhang,[1,*] C. M. Wang,[2,3,†] C. Y. Guo,[4] X. D. Zhu,[1] Y. Zhang,[1] J. Y. Yang,[1] Y. Q. Wang,[1] Z. Qu,[1] L. Pi,[1] Hai-Zhou Lu,[3,5,‡] and M. L. Tian[1,6,7,§]

[1]*Anhui Province Key Laboratory of Condensed Matter Physics at Extreme Conditions, High Magnetic Field Laboratory of the Chinese Academy of Sciences, Hefei 230031, Anhui, China*

[2]*Department of Physics, Shanghai Normal University, Shanghai 200234, China*

[3]*Institute for Quantum Science and Engineering and Department of Physics, Southern University of Science and Technology, Shenzhen 518055, China*

[4]*Institute of Material Science and Engineering, École Polytechnique Fédéral de Lausanne (EPFL), 1015 Lausanne, Switzerland*

[5]*Shenzhen Key Laboratory of Quantum Science and Engineering, Shenzhen 518055, China*

[6]*School of Physics and Materials Sciences, Anhui University, Hefei 230601, Anhui,China*

[7]*Collaborative Innovation Center of Advanced Microstructures, Nanjing University, Nanjing 210093, China*

(Received 14 April 2019; revised manuscript received 14 August 2019; published 6 November 2019)

Thermoelectric effects are more sensitive and promising probes to topological properties of emergent materials, but much less addressed compared to other physical properties. We study the thermoelectric effects of $ZrTe_5$ in a magnetic field. The presence of the nontrivial electrons leads to the anomalous Nernst effect and quasilinear field dependence of thermopower below the quantum limit. In the strong-field quantum limit, both the thermopower and Nernst signal exhibit exotic peaks. At higher magnetic fields, the Nernst signal has a sign reversal at a critical field where the thermopower approaches zero. We propose that these anomalous behaviors can be attributed to the gap closing of the zeroth Landau bands in topological materials with the band inversion. Our understanding to the anomalous thermoelectric properties in $ZrTe_5$ opens a new avenue for exploring Dirac physics in topological materials.

DOI: 10.1103/PhysRevLett.123.196602

Transition-metal pentatellurides ($ZrTe_5$, $HfTe_5$, etc.) have attracted considerable interest as topological materials very close to the boundary of topological phase transition [1–13]. In addition to its nature of multiple topological phases, a moderate magnetic field is enough to drive this layered material into the quantum limit, in which all carriers occupy the lowest Landau band. This provides a platform to explore the exotic quantum phenomena caused by unique band topology in extremely strong magnetic fields. In particular, the magnetoresistance of $ZrTe_5$ decreases drastically when the field exceeds 8 T. Based on the picture of massless Dirac fermions, the sudden drop of magnetoresistance was conjectured to originate either from dynamical mass generation or topological phase transition from a 3D Weyl semimetal to a 2D massive Dirac metal [14,15]. Very recently, in $ZrTe_5$ the 3D quantum Hall effect was observed, which collapses into an exotic insulating state in the extreme quantum limit [16].

In the presence of a perpendicular magnetic field and a longitudinal thermal gradient, the diffusion of carriers can produce a longitudinal electric field $E_x = -S_{xx} \cdot |\nabla T|$ (thermopower) and a transverse electric field $E_y = S_{xy} \cdot |\nabla T|$ (the Nernst effect) [17]. Since these thermoelectric effects are proportional to the derivative of the conductivities, they are more sensitive to anomalous contributions and have been used to study various semimetals and topological materials [18–28]. Zirconium pentatelluride, as a thermoelectric material, has been known for its large thermopower for nearly four decades [29]. Nevertheless, the studies focusing on the thermoelectric properties of $ZrTe_5$ in magnetic fields are rare, especially beyond the quantum limit.

In this Letter, we study the thermopower and Nernst effect of $ZrTe_5$ single crystals. At low temperatures, we observe the anomalous Nernst effect and quasilinear magnetothermopower. When the magnetic field has driven the system in the quantum limit, both the thermopower and Nernst signals present a broad peak which is distinct from quantum oscillations. Intriguingly, further increasing the magnetic field, there is a sign change in S_{xy} at a critical field B^* where $-S_{xx}$ converges to zero. Detailed theoretical analysis shows that such anomalous behaviors can be explained by the gap closing of the zeroth Landau bands. Our study shows that the anomalous thermoelectric effects in and beyond the quantum limit are originated from the 3D Dirac fermions in $ZrTe_5$.

High quality single crystals of $ZrTe_5$ were synthesized using the iodine vapor transport method in a two-zone furnace [30,31]. $-S_{xx}$ and S_{xy} were measured with a standard one-heater-two-thermometers setup in a He^4 cryostat from 1.8 to 300 K. A thermal gradient ∇T was applied along the a axis. The voltage contacts were made by spot welding and each contact resistance was better than 1Ω. In order to

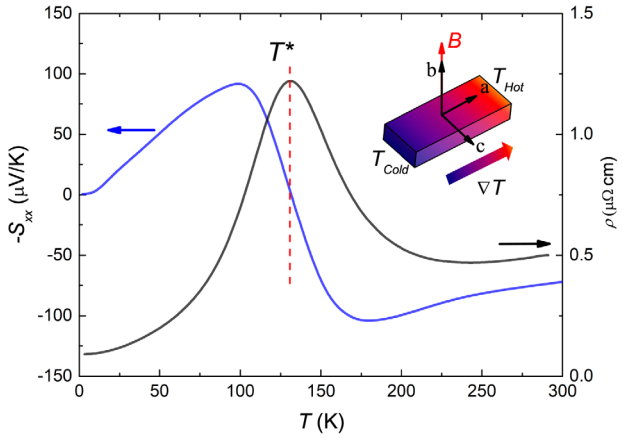

FIG. 1. (a) Temperature dependence of the electrical resistivity $\rho(T)$ (black) and Seebeck coefficient $-S_{xx}(T)$ (blue) of $ZrTe_5$ at zero magnetic field. Inset: the measurement setup. B is the magnetic field and ∇T is the temperature gradient. a, b, and c are crystallographic axes.

exclude the antisymmetric effect in magnetic fields, $-S_{xx}$ and S_{xy} are symmetrized in positive and negative magnetic fields. The high-field measurements up to 33 T were performed at the Chinese High Magnetic Field Laboratory at Hefei using a resistive water-cooled magnet. In the high-field setting, we measured the variation of the voltage produced by a constant heat flow as a function of the magnetic field. The absolute magnitudes of $-S_{xx}$ and S_{xy} were calibrated later in another superconducting magnet. More experimental details are described in the Supplemental Material [31].

Figure 1 presents the temperature dependence of the thermopower $-S_{xx}$. At high temperatures (>132 K), a negative $-S_{xx}$ reveals that the dominant carriers are holes. As temperature decreases, $-S_{xx}$ shifts to positive at around $T^* = 132$ K, where the resistivity shows a peak, indicating that $ZrTe_5$ evolves from a p-type semiconductor to n-type semimetal, consistent with the previous studies [12,37]. Now we turn to investigate the field dependence of $-S_{xx}$ and S_{xy}. As shown in the inset of Fig. 1, the magnetic field is applied along the b axis, perpendicular to the thermal gradient ∇T. At temperatures above the $p-n$ transition, although the dominant carriers are holes, both $-S_{xx}(B)$ and $S_{xy}(B)$ show complex behaviors. Because of the presence of electron- and hole-type charge carriers with different mobilities, $ZrTe_5$ exhibits huge magnetothermopower at T^*, where the thermopower can increase up to 370 μV/K in a field of 9 T. It is larger than those in most materials, but less than those in Weyl semimetals [38]. At temperatures between 30 and 130 K, $-S_{xx}(B)$ can be described by a semiclassical model, i.e., increases rapidly in low-field ($\mu B < 1$) then saturates in high-field limit ($\mu B \gg 1$). $S_{xy}(B)$, on the other hand, manifests a sharp Drude-like peak only at temperatures below 90 K, where the thermally activated hole carriers are undetectable.

As temperature drops below 30 K, both $-S_{xx}(B)$ and $S_{xy}(B)$ tend to deviate from semiclassical expressions. At low temperatures, $-S_{xx}(B)$ even grows quasilinearly with increasing magnetic field up to the quantum limit [31]. Such linear magnetothermopower distinguishes $ZrTe_5$ from other materials [20,21,23,25], which is reminiscent of its linear magnetoresistance. As shown in Fig. 2(e), the low-field $S_{xy}(B)$ evolves from a conventional Drude-like peak to steplike profile with decreasing temperature. Recently, the anomalous Hall effect was claimed in the p-type $ZrTe_5$ ($T^* = 5$ K) [39]. Despite the different carrier types in that and our $ZrTe_5$, the band structure is expected to be intrinsically the same [40]. In this sense, the steplike S_{xy} could be regarded as a signature of the anomalous Nernst effect arising from a nontrivial profile of Berry curvature. Our sample hosts both trivial and nontrivial electrons at low temperatures [14,37]. In order to distinguish the conventional and anomalous Nernst signals, we fit the low-field data by using an empirical formula [25]

$$S_{xy}^{\mathrm{tot}} = S_{xy}^{N}\frac{\mu B}{1+(\mu B)^2} + S_{xy}^{A}\tanh\left(\frac{B}{B_0}\right), \qquad (1)$$

where μ is the carrier mobility and B_0 is the saturation field above which the signal reaches its plateau value. S_{xy}^{N} and S_{xy}^{A} are the amplitudes of the conventional and anomalous Nernst signals, respectively. As displayed in Fig. 2(e), such empirical expressions provide good fits. According to our analysis, the anomalous Nernst signal emerges below 30 K and S_{xy}^{A}/S_{xy}^{N} increases drastically with decreasing temperature [Fig. 2(f)]. At lowest temperature, the magnitudes of the anomalous and conventional Nernst signals are comparable. All results indicate that the nontrivial electrons begin to dominate the magnetothermoelectric properties below 30 K, leading to the unusual behavior of $-S_{xx}(B)$ and $S_{xy}(B)$.

The quantum oscillations of thermoelectric response are strong compared to the background. By employing the fast Fourier transform we obtain only one frequency $F = 5.2$ T, which corresponds to the nontrivial electron pocket around the Γ point [37]. Recent studies show that the integer Landau indices of $ZrTe_5$ can be determined from the peak positions of the resistivity [4,13–16,33]. The oscillation of $-S_{xx}$ is largely in phase with ρ_{xx} [31]. Therefore, the $\nu \geq 2$ Landau levels are marked at the maxima of $-S_{xx}$ in Fig. 2(g). When the magnetic fields reach above 5.2 T, all electrons should occupy the lowest Landau band; i.e., the system is in the quantum limit. In the quantum limit, the thermopower of a Dirac or Weyl semimetal is expected to grow linearly and nonsaturatingly with increasing magnetic field [41]. However, in our cases, $-S_{xx}$ exhibits an unexpected broad peak above 5 T.

In order to further elucidate the unusual thermoelectric response in the quantum limit, we increase the magnetic

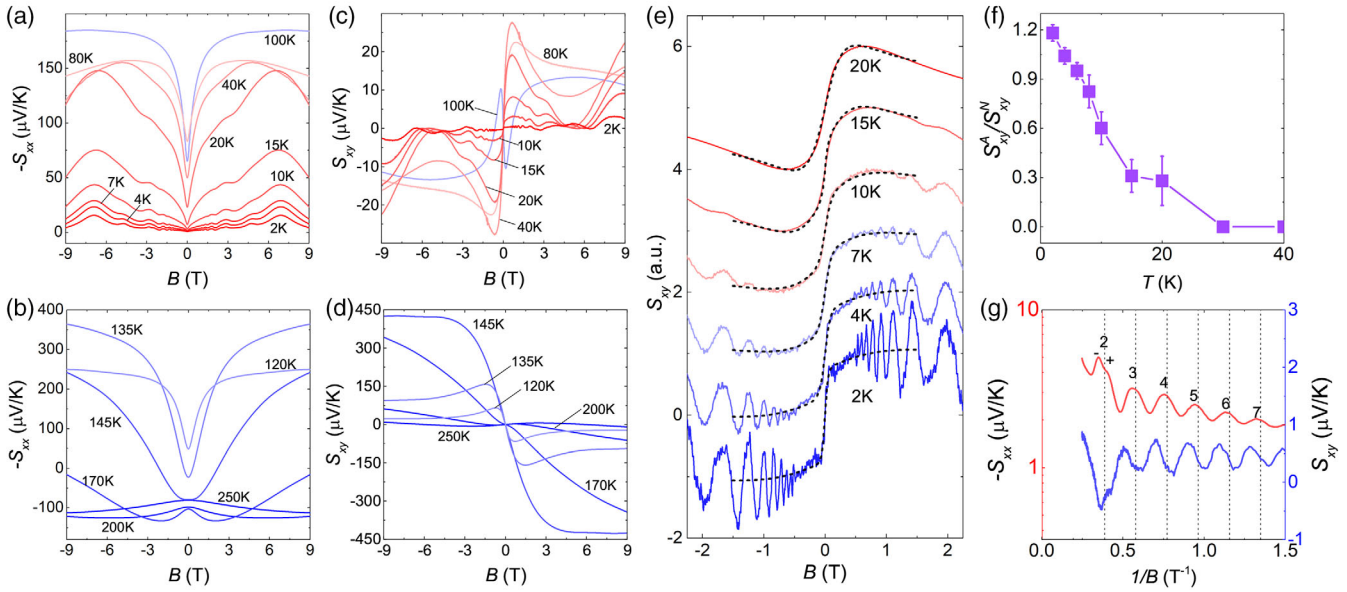

FIG. 2. Magnetic field dependence of the thermopower $-S_{xx}$ (a),(b) and Nernst signal S_{xy} (c),(d) from 1.8 to 300 K. (e) S_{xy} at low fields at several temperatures below 20 K. The data are normalized and shifted for clarity. The black dashed lines represent the fitting with Eq. (1). (f) Temperature dependence of the ratio between the anomalous and conventional Nernst signals S_{xy}^A/S_{xy}^N, which is derived from the fitting curves in (e). (g) $-S_{xx}$ and S_{xy} as functions of $1/B$ at 1.8 K. The integer indices are marked at the maxima of $-S_{xx}$.

field up to 33 T. As shown in Fig. 3(a), $-S_{xx}$ starts to drop around 7 T, then reaches a minimum around 15 T. Further increasing the magnetic field up to 33 T, $-S_{xx}$ turns to increase. Correspondingly, a hump emerges in the Nernst signal S_{xy} right after the system enters the quantum limit. At a first glance, these anomalous features look like part of the quantum oscillation from the Landau bands $(0,+)$ or $(0,-)$. However, the amplitude of the peak is much higher than those of the quantum oscillations. Another anomalous feature is that the Nernst signal S_{xy} changes its sign at around $B^* = 14$ T, where the thermopower $-S_{xx}$ at different temperatures converge to zero. The change of carrier type could lead to a sign reversal in the Nernst or Hall signal. Previously, a field-induced sign change of ρ_{yx} was observed in the Weyl semimetal TaP, in which the lowest Landau band moves above the chemical potential in an extremely strong magnetic field, leading to a dramatic reduction of the carriers in the Weyl electron pockets [42]. However, for our sample, the charge carriers at low temperatures are electrons only, and there is no holelike band near the Fermi level [37]. Moreover, the Hall resistivity ρ_{yx} varies smoothly near B^* [31]. Thus, the change of carrier type is unlikely to explain the anomalous sign reversal of S_{xy}.

We now explore the underlying mechanism for the anomalous $-S_{xx}$ and S_{xy} in the quantum limit. As we discussed above, the nontrivial electrons are the origin of the quantum oscillations and dominate the unusual thermoelectric properties at low temperatures. Hence, our analysis mainly focuses on them. We use a 3D massive Dirac Hamiltonian, which was derived from the low-energy effective $k \cdot p$ Hamiltonian in the presence of the spin-orbit coupling [7]. The Landau bands in a magnetic field along the b axis for index $\nu \geq 1$ are found as

$$E_{\nu s\lambda}(k_z) = s\sqrt{\left(\sqrt{\nu\frac{2eBv^2}{\hbar} + m^2} + s\lambda\frac{g\mu_B B}{2}\right)^2 + v^2k_z^2}, \tag{2}$$

and for $\nu = 0$

$$E_{0s}(k_z) = s\sqrt{\left(m - \frac{g\mu_B B}{2}\right)^2 + v^2k_z^2}, \tag{3}$$

where $s = \pm 1$ represents the electron and hole bands, $\lambda = \pm 1$, v is the Fermi velocity, m is the Dirac mass describing the small gap near the Γ point [1], and g is the g factor [31]. This model has been shown effective to describe the infrared spectroscopy experiment of $ZrTe_5$ in the presence of a strong magnetic field [7]. For simplicity we use an isotropic Fermi velocity, which does not affect transport behaviors qualitatively. For this low-density system, the trivial band at the M point does not influence the thermotransport due to its higher energy and has been excluded from the discussions. We find that the band bottom of the 0th Landau bands reads

$$E_{0s}(0) = s\left|m - \frac{g\mu_B B}{2}\right|. \tag{4}$$

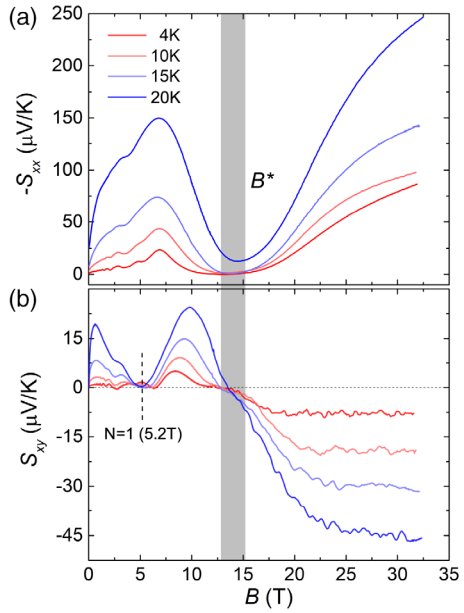

FIG. 3. (a) High-field measurements of $-S_{xx}$ up to 33 T at several temperatures. (b) High-field measurements of S_{xy} at several temperatures. The critical field B^* is indicated by the gray line around 14 T where S_{xy} changes its sign and $-S_{xx}$ converges to zero.

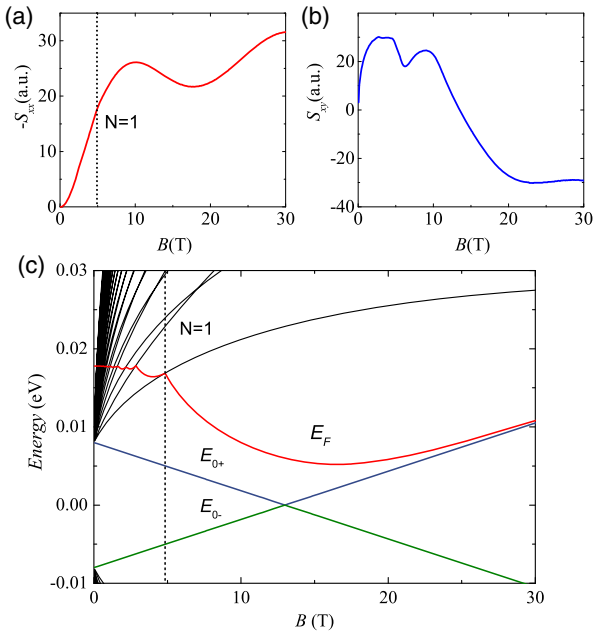

FIG. 4. The calculated (a) $-S_{xx}$ and (b) S_{xy} as functions of the magnetic field. (c) The band bottoms of the Landau bands vs the magnetic field. The blue and green lines are for the 0th bands E_{0+} and E_{0-}. The red line represents the Fermi energy E_F. The parameters are $v = 0.2$ eV nm [16], $m = 0.008$ eV [1], and $g = 21.3$ [14]. The carrier density $n = 4 \times 10^{16}$ cm^{-3}.

Therefore, for a finite mass m, the gap between the 0th electron and hole Landau bands first decreases and then increases with the magnetic field. There is a critical magnetic field $B^* = 2m/g\mu_B$ where the system becomes gapless. This is due to the band inversion, a characteristic of topological materials, different from the trivial ones, where the energy interval between the 0th electron and hole Landau bands increases monotonically with the magnetic field. Because of the small mass and large g factor of $ZrTe_5$, it is easy to observe this Landau-band gap closing at a moderate field. Further, in this low-density system at large magnetic fields, the carrier density is fixed [43]

$$n = \frac{1}{2\pi\ell_B^2}\sum_{k_z}\left(f(E_{0+}) + \sum_{\nu,\lambda} f(E_{\nu+\lambda})\right), \qquad (5)$$

with $f(x)$ being the Fermi-Dirac distribution function. This fixed n leads to the dramatic drop of the Fermi energy beyond the quantum limit due to the gap closing of the 0th Landau bands.

Our numerical results in Fig. 4 confirm the above mechanism. Here all the parameters are from the experiments [14,16] or quantitatively comparable with the first-principles calculation [1]. Before entering the quantum limit, the Fermi energy oscillates around the zero-field value and thermoelectric tensors undergo quantum oscillations as higher Landau bands are depopulated. At $B \simeq 5$ T, the Fermi energy begins to cut only the lowest electron Landau band and the system enters the quantum limit. In contrast to the topologically trivial case and higher Landau bands, the bottoms of the 0th electron and hole Landau bands decreases or increases linearly. They intersect at a field $2m/g\mu_B = 13$ T and separate again at higher fields. Because of the increase of the Landau degeneracy, the Fermi energy drops quickly and shows a minimum near this critical field. Therefore, the density of states and thermopower $-S_{xx}$ show a large dip [31]. It turns out that the thermopower will continue to grow linearly with increasing B in the quantum limit for massless Dirac systems [41], so the latter dip of $-S_{xx}$ results in the anomalous large peak. Moreover, the two terms in the Nernst signal $S_{xy} = \rho_{xx}\alpha_{xy} - \rho_{yx}\alpha_{xx}$ [$\alpha_{\mu\mu'} = (\pi^2 k_B^2 T/3e)\,(\partial\sigma_{\mu\mu'}/\partial\epsilon)|_{\epsilon=E_F}$] have opposite signs. They compete with each other and have the same absolute value when the Landau bands are gapless, resulting in the sign reversal of S_{xy}. A recent observation of a cusplike feature in the magnetoinfrared spectrum around 17 T also agrees well with our mechanism of the 0th Landau band gap closing [5]. Above B^*, the gap of the lowest Laudau bands increases, which leads to the growth in the thermopower.

Note that the quantum oscillations are not clearly visible in Fig. 4(a), because of a strong disorder scattering assumed in our calculation. As a consequence, the calculated $-S_{xx}$ only has a dip near B^* while the experimental $-S_{xx}(B^*)$ converges to zero. Nevertheless, on the basis of our experimental results, $-S_{xx}(B^*) \approx 0$ and sign reversal in

$S_{xy}(B^*)$ are important characteristics of 3D massive Dirac fermions. Similar behavior may be observed in other Dirac Fermions or TIs with small band gap and large g factor [21,44]. We need to emphasize that, due to the significant contribution from those trivial bands, most experimental signatures of the anomaly near B^* are often subtle and indirect. The anomalous thermoelectric effects, on the other hand, are directly attributed to the intrinsic behavior of those nontrivial electrons. In this sense, high-field thermoelectric studies provide a robust, simple, and effective experimental tool to identify the exotic behavior of topological materials.

We acknowledge very helpful discussions with C. L. Zhang, C. Zhang, and L. Jiao. This work was supported by the Natural Science Foundation of China (Grants No. U1932154, No. 11974249, No. U1732274, and No. U1732159); Youth Innovation Promotion Association CAS (Grant No. 2018486); the Innovative Program of Development Foundation of Hefei Center for Physical Science and Technology (Grant No. 2017FXCX001); the Scientific Instrument Developing Project of the Chinese Academy of Sciences (Grant No. YJKYYQ20180059); and the Natural Science Foundation of Shanghai (Grant No. 19ZR1437300). H. Z. L. was supported by the Guangdong Innovative and Entrepreneurial Research Team Program (2016ZT06D348), the National Key R&D Program (2016YFA0301700), the National Natural Science Foundation of China (11574127), and the Science, Technology and Innovation Commission of Shenzhen Municipality (ZDSYS20170303165926217, JCYJ20170412152620376, KYTDPT20181011104202253). The numerical calculations were supported by the Center for Computational Science and Engineering of Southern University of Science and Technology.

*Corresponding author.
zhangjinglei@hmfl.ac.cn
†Corresponding author.
wangcm@shnu.edu.cn
‡Corresponding author.
luhz@sustech.edu.cn
§Corresponding author.
tianml@hmfl.ac.cn

[1] H. M. Weng, X. Dai, and Z. Fang, Phys. Rev. X **4**, 011002 (2014).
[2] Q. Li, D. E. Kharzeev, C. Zhang, Y. Huang, I. Pletikosic, A. V. Fedorov, R. D. Zhong, J. A. Schneeloch, G. D. Gu, and T. Valla, Nat. Phys. **12**, 550 (2016).
[3] G. L. Zheng, J. W. Lu, X. D. Zhu, W. Ning, Y. Y. Han, H. W. Zhang, J. L. Zhang, C. Y. Xi, J. Y. Yang, H. F. Du, K. Yang, Y. H. Zhang, and M. L. Tian, Phys. Rev. B **93**, 115414 (2016).
[4] X. Yuan, C. Zhang, Y. Liu, C. Y. Song, S. D. Shen, X. Sui, J. Xu, H. Yu, Z. An, J. Zhao, H. Yan, and F. X. Xiu, NPG Asia Mater. **8**, e325 (2016).
[5] Z. G. Chen, R. Y. Chen, R. D. Zhong, J. Schneeloch, C. Zhang, Y. Huang, F. Qu, R. Yu, Q. Li, G. D. Gu *et al.*, Proc. Natl. Acad. Sci. U.S.A. **114**, 816 (2017).
[6] R. Y. Chen, S. J. Zhang, J. A. Schneeloch, C. Zhang, Q. Li, G. D. Gu, and N. L. Wang, Phys. Rev. B **92**, 075107 (2015).
[7] R. Y. Chen, Z. G. Chen, X.-Y. Song, J. A. Schneeloch, G. D. Gu, F. Wang, and N. L. Wang, Phys. Rev. Lett. **115**, 176404 (2015).
[8] R. Wu, J. Z. Ma, S. M. Nie, L. X. Zhao, X. Huang, J. X. Yin, B. B. Fu, P. Richard, G. F. Chen, Z. Fang *et al.*, Phys. Rev. X **6**, 021017 (2016).
[9] X. B. Li, W. K. Huang, Y. Y. Lv, K. W. Zhang, C. L. Yang, B. B. Zhang, Y. B. Chen, S. H. Yao, J. Zhou, M. H. Lu *et al.*, Phys. Rev. Lett. **116**, 176803 (2016).
[10] H. Xiong, J. A. Sobota, S.-L. Yang, H. Soifer, A. Gauthier, M.-H. Lu, Y.-Y. Lv, S.-H. Yao, D. Lu, M. Hashimoto, P. S. Kirchmann, Y.-F. Chen, and Z.-X. Shen, Phys. Rev. B **95**, 195119 (2017).
[11] G. Manzoni, L. Gragnaniello, G. Autes, T. Kuhn, A. Sterzi, F. Cilento, M. Zacchigna, V. Enenkel, I. Vobornik, L. Barba *et al.*, Phys. Rev. Lett. **117**, 237601 (2016).
[12] B. Xu, L. X. Zhao, P. Marsik, E. Sheveleva, F. Lyzwa, Y. M. Dai, G. F. Chen, X. G. Qiu, and C. Bernhard, Phys. Rev. Lett. **121**, 187401 (2018).
[13] J. L. Zhang, C. Y. Guo, X. D. Zhu, L. Ma, G. L. Zheng, Y. Q. Wang, L. Pi, Y. Chen, H. Q. Yuan, and M. L. Tian, Phys. Rev. Lett. **118**, 206601 (2017).
[14] Y. W. Liu, X. Yuan, C. Zhang, Z. Jin, A. Narayan, C. Luo, Z. G. Chen, L. Yang, J. Zou, X. Wu, S. Sanvito, Z. C. Xia, L. Li, Z. Wang, and F. X. Xiu, Nat. Commun. **7**, 12516 (2016).
[15] G. L. Zheng, X. D. Zhu, Y. Q. Liu, J. W. Lu, W. Ning, H. W. Zhang, W. S. Gao, Y. Y. Han, J. Y. Yang, H. F. Du *et al.*, Phys. Rev. B **96**, 121401(R) (2017).
[16] F. D. Tang, Y. F Ren, P. P. Wang, R. D. Zhong, J. Schneeloch, S. Y. Yang, K. Yang, P. Lee, G. D. Gu, Z. H. Qiao, and L. Y. Zhang, Nature (London) **569**, 537 (2019).
[17] K. Behnia and H. Aubin, Rep. Prog. Phys. **79**, 046502 (2016).
[18] K. Behnia, M.-A. Méasson, and Y. Kopelevich, Phys. Rev. Lett. **98**, 166602 (2007).
[19] B. Fauqué, Z. Zhu, T. Murphy, and K. Behnia, Phys. Rev. Lett. **106**, 246405 (2011).
[20] B. Fauqué, N. P. Butch, P. Syers, J. Paglione, S. Wiedmann, A. Collaudin, B. Grena, U. Zeitler, and K. Behnia, Phys. Rev. B **87**, 035133 (2013).
[21] T. Liang, Q. Gibson, J. Xiong, M. Hirschberger, S. P. Koduvayur, R. J. Cava, and N. P. Ong, Nat. Commun. **4**, 2696 (2013).
[22] Z. Zhu, X. Lin, J. Liu, B. Fauque, Q. Tao, C. Yang, Y. Shi, and K. Behnia, Phys. Rev. Lett. **114**, 176601 (2015).
[23] Z. Z. Jia, C. Z. Li, X. Q. Li, J. R. Shi, Z. M. Liao, D. P. Yu, and X. S. Wu, Nat. Commun. **7**, 13013 (2016).
[24] J. Gooth, A. C. Niemann, T. Meng, A. G. Grushin, K. Landsteiner, B. Gotsmann, F. Menges, M. Schmidt, C. Shekhar, V. Süβ *et al.*, Nature (London) **547**, 324 (2017).
[25] T. Liang, J. J. Lin, Q. Gibson, T. Gao, M. Hirschberger, M. H. Liu, R. J. Cava, and N. P. Ong, Phys. Rev. Lett. **118**, 136601 (2017).

[26] X. K. Li, L. C. Xu, L. C. Ding, J. H. Wang, M. S. Shen, X. F. Lu, Z. W. Zhu, and K. Behnia, Phys. Lett. **119A**, 056601 (2017).
[27] M. Matusiak, J. R. Cooper, and D. Kaczorowski, Nat. Commun. **8**, 15219 (2017).
[28] S. J. Watzman, T. M. McCormick, C. Shekhar, S.-C. Wu, Y. Sun, A. Prakash, C. Felser, N. Trivedi, and J. P. Heremans, Phys. Rev. B **97**, 161404(R) (2018).
[29] T. E. Jones, W. W. Fuller, T. J. Wieting, and F. Levy, Solid State Commun. **42**, 793 (1982).
[30] G. N. Kamm, D. J. Gillespie, A. C. Ehrlich, T. J. Wieting, and F. Levy, Phys. Rev. B **31**, 7617 (1985).
[31] See Supplemental Material at http://link.aps.org/supplemental/10.1103/PhysRevLett.123.196602, which includes Refs. [32–36], for the experimental methods, fitting of $-S_{xx}$ and S_{xy}, quantum oscillation of $-S_{xx}$ and S_{xy}, high-field studies for ρ_{xx} and ρ_{xy}, and theory of the thermopower and Nernst effect for $ZrTe_5$.
[32] B. L. Brandt, D. W. Liu, and L. G. Rubin, Rev. Sci. Instrum. **70**, 104 (1999).
[33] J. Y. Wang, J. J. Niu, B. M. Yan, X. Q. Li, R. Bi, Y. Yao, D. P. Yu, and X. S. Wu, Proc. Natl. Acad. Sci. U.S.A. **115**, 9145 (2018).
[34] H. Z. Lu, S. B. Zhang, and S. Q. Shen, Phys. Rev. B **92**, 045203 (2015).
[35] P. Goswami, J. H. Pixley, and S. Das Sarma, Phys. Rev. B **92**, 075205 (2015).
[36] S.-B. Zhang, H.-Z. Lu, and S.-Q. Shen, New J. Phys. **18**, 053039 (2016).
[37] Y. Zhang, C. Wang, L. Yu, G. Liu, A. Liang, J. Huang, S. Nie, Y. Zhang, B. Shen, J. Liu *et al.*, Nat. Commun. **8**, 15512 (2017).
[38] U. Stockert, R. D. dos Reis, M. O. Ajeesh, S. J. Watzman, M. Schmidt, C. Shekhar, J. P. Heremans, C. Felser, M. Baenitz, and M. Nicklas, J. Phys. Condens. Matter **29**, 325701 (2017).
[39] T. Liang, J. J. Lin, Q. Gibson, S. Kushwaha, M. H. Liu, W. D. Wang, H. Y. Xiong, J. A. Sobota, M. Hashimoto, P. S. Kirchmann *et al.*, Nat. Phys. **14**, 451 (2018).
[40] P. Shahi, D. J. Singh, J. P. Sun, L. X. Zhao, G. F. Chen, Y. Y. Lv, J. Li, J. Q. Yan, D. G. Mandrus, and J. G. Cheng, Phys. Rev. X **8**, 021055 (2018).
[41] B. Skinner and L. Fu, Sci. Adv. **4**, eaat2621 (2018).
[42] C. L. Zhang, S. Y. Xu, C. M. Wang, Z. Lin, Z. Z. Du, C. Guo, C. C. Lee, H. Lu, Y. Feng, S.-M. Huang *et al.*, Nat. Phys. **13**, 979 (2017).
[43] C. L. Zhang, C. M. Wang, Z. Yuan, C. C. Lee, L. Pi, C. Xi, H. Lin, N. Harrison, H. Z. Lu, J. Zhang, and S. Jia, Nat. Commun. **10**, 1028 (2019).
[44] B. A. Assaf, T. Phuphachong, E. Kampert, V. V. Volobuev, P. S. Mandal, and J. Sánchez-Barriga, O. Rader, G. Bauer, G. Springholz, L. A. de Vaulchier, and Y. Guldner, Phys. Rev. Lett. **119**, 106602 (2017).